# Trapping of Intact, Singly-Charged, Bovine Serum Albumin Ions Injected from the Atmosphere with a 10-cm Diameter, Frequency-Adjusted Linear Quadrupole Ion Trap

Hideya Koizumi, William B. Whitten, and Peter T. A. Reilly
Oak Ridge National Laboratory, Oak Ridge, Tennessee, USA

High-resolution real-time particle mass measurements have not been achievable because the enormous amount of kinetic energy imparted to the particles upon expansion into vacuum competes with and overwhelms the forces applied to the charged particles within the mass spectrometer. It is possible to reduce the kinetic energy of a collimated particulate ion beam through collisions with a buffer gas while radially constraining their motion using a quadrupole guide or trap over a limited mass range. Controlling the pressure drop of the final expansion into a quadrupole trap permits a much broader mass range at the cost of sacrificing collimation. To achieve high-resolution mass analysis of massive particulate ions, an efficient trap with a large tolerance for radial divergence of the injected ions was developed that permits trapping a large range of ions for on-demand injection into an awaiting mass analyzer. The design specifications required that frequency of the trapping potential be adjustable to cover a large mass range and the trap radius be increased to increase the tolerance to divergent ion injection. The large-radius linear quadrupole ion trap was demonstrated by trapping singly-charged bovine serum albumin ions for on-demand injection into a mass analyzer. Additionally, this work demonstrates the ability to measure an electrophoretic mobility cross section (or ion mobility) of singly-charged intact proteins in the low-pressure regime. This work represents a large step toward the goal of high-resolution analysis of intact proteins, RNA, DNA, and viruses. (J Am Soc Mass Spectrom 2008, 19, 1942–1947) © 2008 Published by Elsevier Inc. on behalf of American Society for Mass Spectrometry

Ever since the mass spectrometer was introduced, scientists have looked for ways to increase the mass range. The greatest advances came with the introduction of electrospray ionization (ESI) [1] and matrix-assisted laser desorption ionization (MALDI) [2]. These techniques permitted the production of massive ions in vacuum for subsequent mass analysis. Yet even with the advance of large ion production into the megadalton (MDa) range, the working range of mass spectrometers remained in the tens of kilodalton (kDa) range. The working range defines the range of mass-to-charge ratios where the spectrometer yields the most useful information; in other words, the range with the highest resolution, sensitivity, and mass accuracy.

The working range limitation results from the kinetic energy imparted to the large ions during expansion into vacuum. Liu et al. [3] measured the centerline velocity of particles exiting their aerodynamic lens system through a 2-Torr expansion into vacuum. By extrapolating their results to zero particle diameter (mass), the kinetic energy of the particles traveling along the centerline of the expansion was found to be roughly linear yielding ~13.5, 85.3, and 530 eV for 10, 100, and 1000 kDa molecules. This result shows that even a low-pressure expansion can impart enough kinetic energy into large ions to compete with and eventually overwhelm the typically applied fields as a function of increasing ion mass. Larger pressure drops exacerbate the problem.

It is natural to suggest that the kinetic energy of ions in the 100 eV range can be compensated for by applying an electric field to reduce the forward velocity. It is true that application of an electric field can reduce the velocity of an ion to near zero, but only in one direction and not compensating for the spread of kinetic energy that increases with increasing mass. Beavis and Chait [4] showed that the ion velocity distribution does not change as a function of ion mass during MALDI expansion into vacuum. Generally, the velocity peaks between 600 and 800 $ms^{-1}$ and ranges from a minimum near 200 $ms^{-1}$ to a maximum near 1400 $ms^{-1}$. The kinetic energy of 10, 100, and 1000 kDa particles moving

Address reprint requests to Dr. Peter T. A. Reilly, Oak Ridge National Laboratory, P.O. Box 2008, MS 6142, Oak Ridge, TN 37831, USA. E-mail: ReillyPT@ornl.gov


1044-0305/08/$32.00
doi:10.1016/j.jasms.2008.08.007

Published online August 15, 2008
Received June 11, 2008
Revised August 11, 2008
Accepted August 11, 2008

at 700 $ms^{-1}$ is ~25, 250, and 2500 eV, respectively, but the range of kinetic energies for these same particles defined at limits of the velocity distribution are 100, 1000, and 10,000 eV, respectively. This kinetic energy spread reveals the reason for the loss of resolution in MALDI experiments as a function of increasing mass. Consequently, high-resolution mass analysis above ~20 kDa requires that the expansion-induced kinetic energy be reduced as much as possible.

It was the aerodynamics of the expansion that created the velocity distribution of the particulate ions; therefore, aerodynamics is the most likely place to look for a solution to remove the expansion-induced kinetic energy. The simplest solution is to pass the energetic ions through a buffer gas inside a linear quadrupole trap. Quadrupole traps are preferred because they are better at focusing the ions on the central axis relative to higher order multipoles. The ions can then be trapped by applying potentials to the endcap electrodes. Dropping the potential of the endcap will permit on-demand ejection of the ions with a controllable amount of field-created kinetic energy from the quadrupole trap into a mass analyzer for high-resolution analysis. The typical linear quadrupole trap or ion guide design requires the input of a well-collimated particulate ion beam for efficient trapping. The expansion required to create a collimated beam limits the trapping mass range. Controlling the pressure drop of the final expansion into the quadrupole ion trap can be used to reduce kinetic energy and increase the mass range at the cost of collimation. For this reason, a linear quadrupole ion trap that was tolerant of injected ion dispersion was designed and tested using a collimated particulate ion beam generated with an aerodynamic lens-based inlet. This work documents our effort in developing an ion trap for catching large mass-to-charge ratio ions that were injected into vacuum from the atmosphere with the eventual goal of holding them for subsequent injection into an awaiting analyzer. It is the first large step toward direct high-resolution mass analysis of intact proteins, RNA, DNA, and viruses.

## Stopping Particulate Ions with a Buffer Gas

The stopping distance is the finite distance a particle travels before coming to rest after it has been projected into a stationary fluid with some initial velocity [5]. It is defined by the following equation:

$$S = V_0 \rho_p d_p^2 C_c / 18\eta \quad (1)$$

where $V_0$ is the initial velocity, $\rho_p$ is the particle density, $d_p$ is the particle diameter, $C_c$ is the Cunningham slip correction factor and $\eta$ is the viscosity. The Cunningham slip correction factor is given by [5]:

$$C_c = 1 + \frac{\left(1539 + 7.51e^{-0.0741Pd_p}\right)}{Pd_p} \quad (2)$$

for solid particles, where P is the pressure in kPa and $d_P$ is the particle diameter in $\mu$m. The initial velocity, $V_0$ ($ms^{-1}$), was calculated by extrapolation of the particle velocity function determined by Liu et al. [3] for a 2-Torr final expansion from an aerodynamic lens system:

$$V_0 = 88.6\left(\rho_p d_p\right)^{-0.304} \quad (3)$$

Here $\rho_p$ is in units of $g/cm^3$ and $d_p$ is in $\mu$m. The results in Figure 1 show that particles up to 20 nm in diameter can be stopped in a quadrupole trap less than 40 cm long with buffer gas pressures at 20 mTorr. For reference, a 20 nm size particle with a density of 1 $g/cm^3$ has a mass of ~2.5 MDa. Coupling an aerodynamic lens inlet/gas-filled linear quadrupole trap combination with a time-of-flight or digital ion trap mass analyzer would permit trapping and mass analysis of particles covering the entire range of proteins and protein complexes, suggesting the possibility of high-resolution mass analysis of intact proteins.

## Design of a Linear Quadrupole Trap for Particulate Ions

The ultimate goal of our work is to provide efficient trapping and storage of ions over a mass range that contains viruses (up to 10 GDa) so that they can then be injected into an awaiting mass analyzer. The trapping efficiency and mass range will increase with the linear trap radius provided the final expansion can be controlled. The larger radius (5 cm) enables higher capture efficiencies because ions with larger off-axis initial kinetic energy can be trapped as a result of the in-

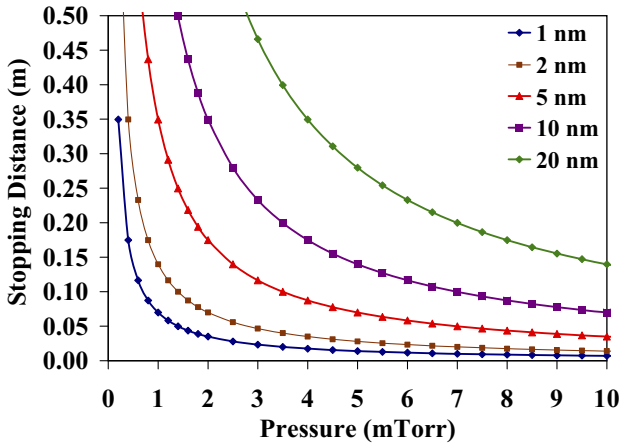


**Figure 1.** Stopping distance as a function of pressure for a range of particle sizes from 1 to 50 nm. Particle size assumes unit density and spherical shape. (1 nm = 330 Da, 2 nm = 2.5 kDa, 5 nm = 39.5 kDa, 10 nm = 330 kDa, and 20 nm = 2.5 MDa.)

creased available radial stopping distance. It is desirable to maximize the radius while minimizing the volume of the device. Fortunately, an appropriate design was illustrated in Dawson's text [6], with the original work by Hayashi and Sakudo [7]. Hyperbolic fields can be achieved with circular concave structures. The potential contours and the *xy*-cross sectional structure of the device are illustrated in Figure 2a. The circular concave electrode structure is much more volume-efficient than large diameter round rods, while supplying uniform hyperbolic fields. The potential contour structure close to the endcaps is illustrated in the *xz*-cross sectional view in Figure 2b. This design keeps the fringe fields away from the center of the device where the ions are trapped. It also permits much better endcap field penetration into the center of the quadrupole trap. Figure 2b reveals the potential contour plot of the entire *xz*-cross section when the potential of the left endcap is dropped to permit ion ejection. This simulation shows that the extraction fields from the endcap penetrate deeply into the quadrupole trap resulting in efficient ion ejection. Additionally, the trajectories of the ejecting ions should not be significantly affected by the fringe fields from the ends of the electrodes.

Increasing the radius of the quadrupole trap used for trapping massive ions has other benefits besides reducing the fringe interaction. The linear quadrupole ion trap is operated digitally with the potentials generated using a FET-based pulser [8]. These pulsers are limited in the amount of power that they can dissipate in the form of heat. The power load is proportional to the frequency times the voltage squared. Increasing the radius reduces the operational frequency of the quadrupole trap by the same factor thereby permitting the use of correspondingly higher voltages or permitting the analysis of smaller ions. Finally, because our ultimate goal is to capture ions in the gigadalton range and higher, it may be possible to control the final pressure drop of the expansion into the large quadrupole trap at the sacrifice of the collimation provided by the aerodynamic lens system.

The large radius quadrupole trap was designed to fit into a 5 in. o.d. tube. The electrodes were longitudinally cut at a 35.8° angle from another 5 in. o.d. tube then

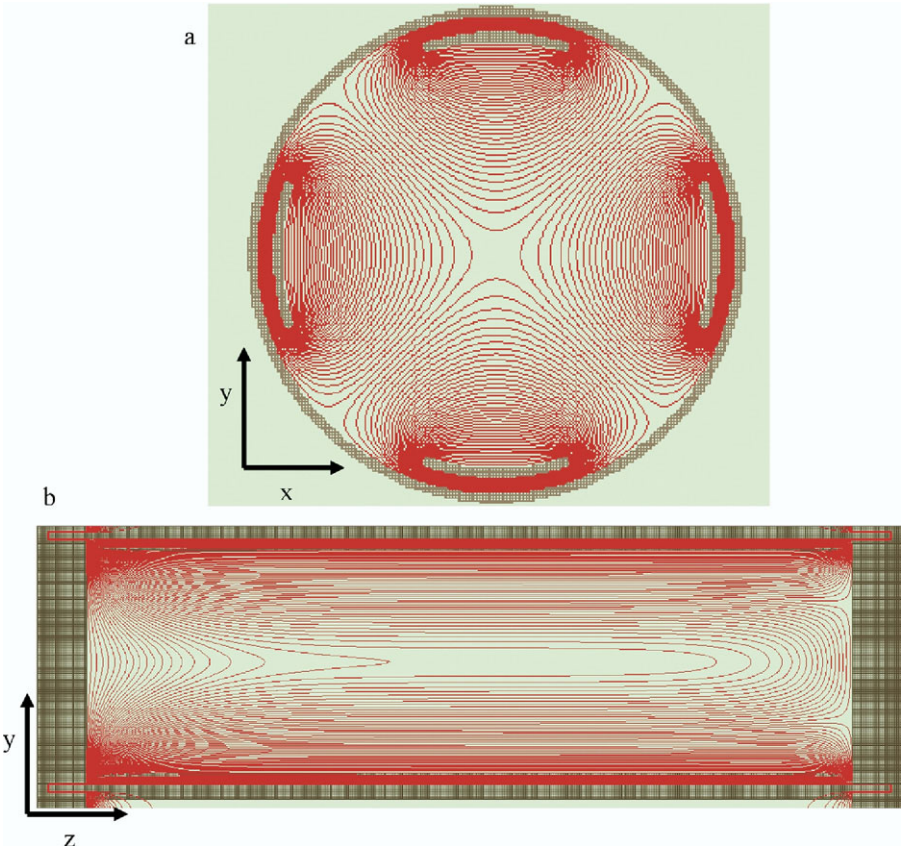


**Figure 2.** SIMION (version 7.0) voltage contour plots for a 10-cm diameter, 35-cm long LQIT with circular concave quadrupole electrodes and 3-cm apertures in the planar entrance and exit electrodes. Contour lines are depicted at every 10 V change in potential; (**a**) xy-cross section of the large radius device with field potential contours suggested for trapping large ions; (**b**) xz-cross sectional view and potential contour plot of the large radius quadrupole with the left-hand endcap potential drop to eject the ions. The fringe field contour structure near the endcap electrodes of a large radius circular concave quadrupole device is also depicted.

milled to length. The electrodes were mounted inside the 5 in. o.d. tube with 1/8 in. insulating spacers. The distance between opposing electrodes is 10.85 cm. The distance between the endcap surfaces is 33.82 cm.

## Experimental

A schematic of the trapping system is shown in Figure 3. It consists of an aerodynamic lens system based on the design of Wang et al. [9], a digitally-operated, gas-filled, quadrupole ion trap, endcap electrodes, and a detector system that incorporated a conversion dynode. The system was oriented in the vertical direction as depicted in the schematic so that the force of gravity acted along the axis of the quadrupole trap. The aerodynamic lens system created a well-collimated beam for particles with diameters less than 30 nm. The carrier gas was air. The distance between the entrance of the skimmer and the front surface of the exit endcap electrode was ~40 cm. The radius of the trap was ~5 cm. The quadrupole trap chamber was backfilled with nitrogen at 5 to 20 mTorr pressure. The analyte chosen for these experiments was bovine serum albumin (BSA) (Sigma) with a molecular weight of ~66 kDa and an electrophoretic mobility diameter of 7.1 nm. The BSA was electrosprayed from a 50/50 solution of ethanol and water. The BSA aerosol impacted the inside surface of the 1/4 in. tube before the 100 $\mu$m inlet orifice. Deliberately interacting the highly-charged aerosol droplets with the grounded metal surface reduced the charge distribution of the BSA-containing droplets before they entered the aerodynamic lens. The particulate ions were collimated by the aerodynamic lens as the carrier gas expanded. After the final expansion, the particle beam passed through a skimmer into the LR-LQIT chamber. By the time the particles entered the chamber, they were fairly dry. Reduction of the BSA charge distribution and the solvent content of the particles were confirmed through experiments discussed in the next section.

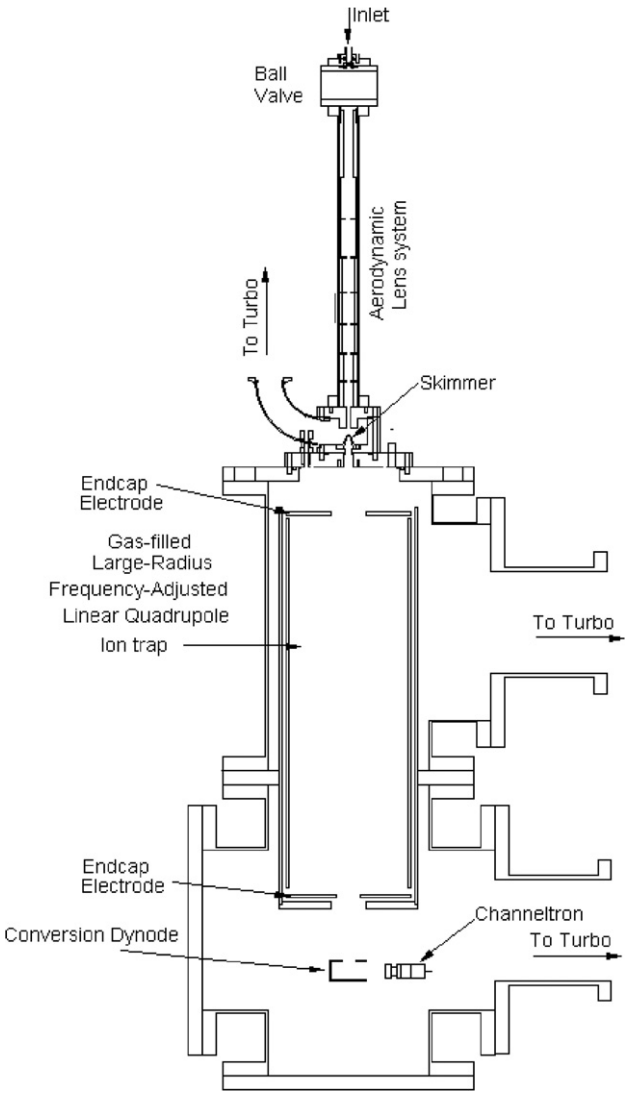


**Figure 3.** The schematic of the large-radius, frequency-adjusted, linear quadrupole ion trap for massive ions. An aerodynamic lens inlet system is used to transmit the particulate ions in a collimated beam into the linear quadrupole ion trap chamber. The large radius, linear quadrupole ion trap is 10-cm in diameter and 35-cm long. The quadrupole electrodes are circular concave and provide a quadrupole field along the trap's central axis. The endcap electrodes were ~11-cm diameter plates with 3-cm apertures. The detector comprised of a 10 kV conversion dynode and a channeltron electron multiplier.

## Results and Discussion

The LR-LQIT was tested by electrospraying BSA into the inlet. The spray was directed onto the inside surface of the tube in front of the 100-$\mu$m diameter orifice to reduce the charge on the droplets. Ions were detected without buffer gas in the chamber or energizing the LR-LQIT. Filling the chamber with $N_2$ at 9 mTorr quenched the ion signal. Turning on the LR-LQIT (700 $V_{0\text{-}p}$, 8 kHz) restored the detected ions. Applying a 65 V positive potential to the entrance endcap electrode reduced the ion signal to zero. The kinetic energy of 7.1-nm, 66 kDa particles from an aerodynamic lens is 62 eV, according to the particle velocity function determined by Liu et al. [3] This sets the upper kinetic energy limit of ions exiting the aerodynamic lens. Individual BSA particles with one charge or more are repelled by a 65 V potential. Singly-charged ions that are multimers or that have substantial amounts of solvent associated with them would not be stopped by the 65 V potential. Setting the frequency of the LR-LQIT to 8000 Hz at 700 $V_{0\text{-}p}$ yielded the largest flux of detected ions. Ions passing through the quadrupole field have a low mass cut-off of ~51 kDa. These results indicate that the majority of ions exiting the aerodynamic lens system are relatively dry, singly-charged, individual BSA molecules.

The LR-LQIT frequency was set to 8000 Hz, and the entrance and exit endcaps were set to +50 and 90 V,

respectively. No signal was observed at the detector under these conditions. Ions were collected in the trap for 4 s, and then the potential of the exit endcap electrode was dropped to −100 V. The oscilloscope was triggered by the endcap voltage drop, and the signal at the detector was recorded as a function of time (see Figure 4). The signal rapidly rose after approximately a 5 ms delay, whereupon the detector saturated for ~2 ms, then decayed to the baseline in about an additional 2 ms.

To demonstrate that the signal resulted from trapped ions, the ejection profile was measured as a function of extraction voltage. Additionally, to reduce the number of BSA ions and to keep the detector from saturating, the LR-LQIT frequency was adjusted to 30 KHz. This reduced the $q$ value of the singly-charged BSA ions to 0.039 yielding a well depth of 5.4 V. The ejection profiles measured with extraction voltages of −50, −100, and −200 V are shown in Figure 5. The brown trace represents the profile of the gate pulse used to switch the exit endcap electrode potential. Increasing the extraction voltage reduced the ejection delay time and narrowed the ejection profile as expected for trapped ions.

Note that the ion flight times are significantly (~10×) longer than what would occur under high vacuum conditions because of the high buffer gas ($N_2$) pressure. One may obtain the reduced ion mobility, $K_0$, related to ion-neutral collisions using the following relation [10]:

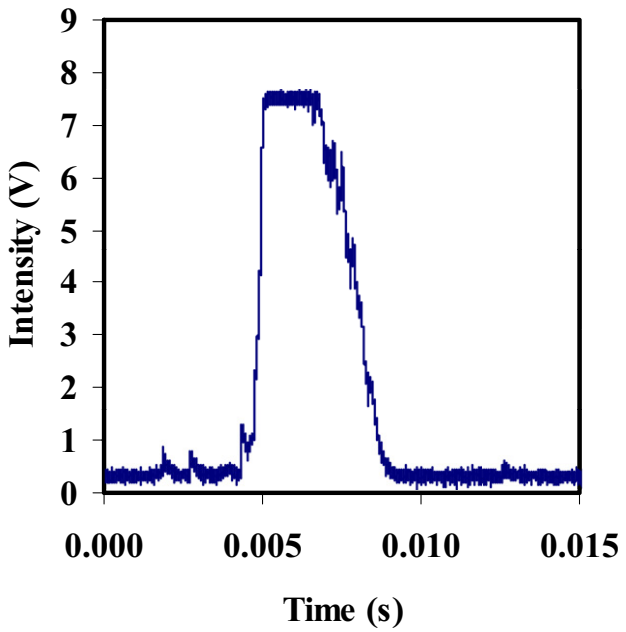


**Figure 4.** Temporal profile of the first ejection of BSA ions from the LR-LQIT trap. The small abundance peaks at shorter flight times are due to individual BSA ions that are continuously injected into the trap during the ejection process that have not been trapped.

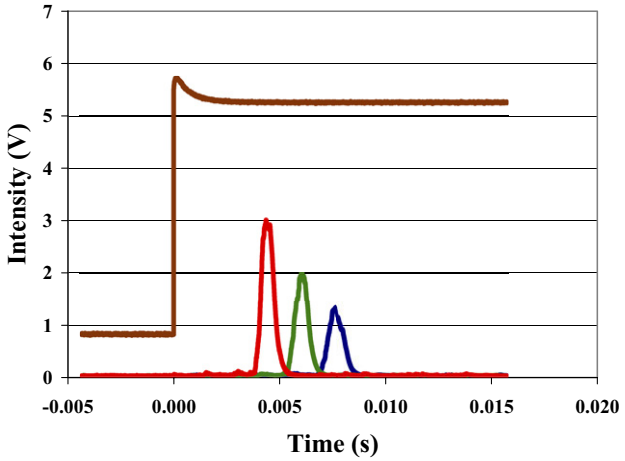


**Figure 5.** The ejection of trapped BSA ions as a function of extraction voltage: −50 (blue), −100 (green), and −200 V (red). The area under the three curves is the same; however the ejection time is different because the extraction potential was changed. The brown trace is the profile of the TTL gate pulse that triggers the changes the endcap potential. All traces are on the same scale.

$$K_0 = \left(\frac{273K}{T}\right)\left(\frac{P}{760Torr}\right)\frac{L^2}{Vt} \tag{4}$$

where V, L, P, T, are voltage drop (V), drift length (cm), pressure (Torr), and temperature (K), respectively. This assumes that the electric field over the path of the ions is constant. The resulting ion mobility of BSA is 1300 $cm^2V^{-1}s^{-1}$ ± 10%. The equation governing gas-phase ion transport in an electric field is given by [10]:

$$K = \frac{3q}{16N}\left(\frac{2\pi}{\mu kT}\right)^{1/2}\frac{1}{\Omega} \tag{5}$$

where K, N, q, $\mu$, k, $\Omega$ are the ion mobility, the number density of the buffer gas molecules, charge on the ion, reduced mass, Boltzmann's constant, and ion cross section, respectively. A hard sphere cross-section for singly-charged BSA of 3900 Å [2] ± 10% was obtained. BSA has a reported electrophoretic mobility diameter of 7.1 nm [11] yielding a cross section of 3960 $Å^2$. The agreement is better than expected because the electric fields and volume flow of carrier gas were not optimized. The mobility resolution of the device could be improved by careful attention to the setup of the applied fields. By judicious selection of the ion gate, this inlet could be used as a structural selection device because different ion mobilities indicate different structures for the same protein.

The BSA ion ejection profiles (at 30 kHz operating frequency) were measured as a function of injection time as shown in Figure 6. The injection times measured were 2 s (green), 4 s (red), and 9 s (blue). The area under the profiles increased linearly with injection time (see inset, Figure 6). The linearity indicates that the ion injection rate was constant and that ion losses were not significant on

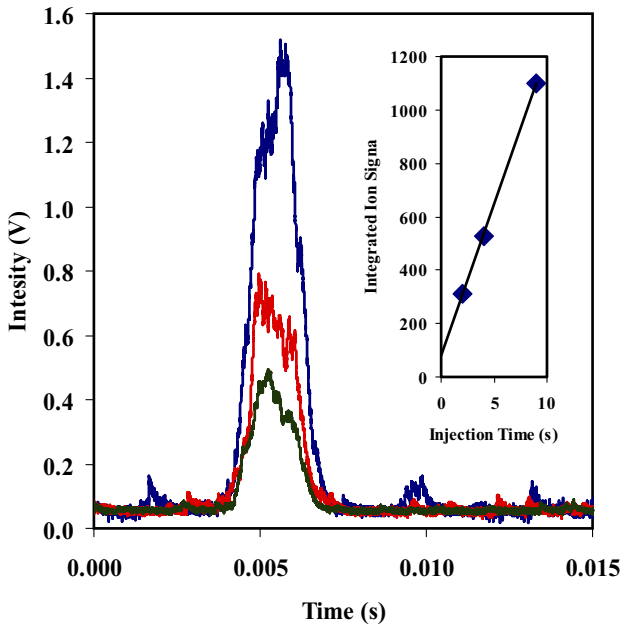


**Figure 6.** BSA ion ejection profiles at 2 s (green), 4 s (red), and 9 s (blue) injection time at q = 0.039. (Inset) Integrated BSA ion signal as a function of injection time. The small abundance peaks at shorter flight times are due to individual BSA ions that are continuously injected into the trap during the ejection process that have not been trapped.

the 10 s time scale, even though the pseudo-potential well depth was not particularly high (5.4 V) [12]. Ion loss at higher values of $q$ should be much less significant. These results suggest that massive ions can be trapped in large quantities and stored for long periods without significant ion loss. Just as importantly, a large number of massive trapped ions can be ejected from the LR-LQIT into an awaiting analyzer with a controlled amount of kinetic energy in a relatively short pulse.

## Conclusions

A large-radius linear quadrupole ion trap was demonstrated to be capable of trapping and holding massive singly-charged ions. This trap can operate at any mass-to-charge ratio if the ions are injected into the trap with low enough kinetic energy so that they are stopped by collisions with a buffer gas before they traverse the trap boundaries. Trapping large ions with a small radius LQIT has been attempted in our laboratory without success. Our previous work revealed that collimating and even stopping the ions in the trap is rather easy. Holding them and ejecting them on-demand is not. To demonstrate the trap, the largest (inexpensive) protein, BSA, which could be stopped at 10 mTorr by buffer gas collisions (see Figure 1), was used. The large radius of the trap makes holding and ejecting the ions on-demand possible. Any other sized particulate ion can be trapped just as well by merely adjusting the trap frequency, provided its kinetic energy entering the trap is not greater than the trap's well depth.

It was also demonstrated that measurement of ion mobility is possible with this ion trap for large particulate ions at low pressures. However, use of this trapping configuration for the purpose of mobility measurements needs further investigation and better design.

The potential of the LR-LQIT has not been fully realized here. Injecting ions as a collimated beam does not fully utilize the LR-LQIT capability because it was developed to efficiently trap ions with large off-axis momentum components. Our next step is to reduce the pressure drop of the expansion into the LR-LQIT so that much larger, minimally charged ions can be trapped. Reducing the pressure drop of the expansion will increase the dispersion of the ions as they enter the quadrupole trap, and will also decrease their kinetic energy. The LR-LQIT was designed for this scenario. Controlling expansions of ions as they move from atmosphere to vacuum is the key to efficiently injecting singly-charged particulate ions with geometric diameters in the hundreds of nm range; this results in a sufficiently low kinetic energy distribution for them to be stopped by buffer gas collisions inside the quadrupole trap and then trapped for subsequent injection into a mass analyzer. This is one of the primary requirements for extending the working range of mass spectrometers so that viruses and other massive biological species can eventually be mass analyzed in an intact form.

## Acknowledgments

The authors acknowledge funding for this research by the U.S. Department of Energy, Office of Nonproliferation Research and Engineering, under contract no. DE-AC05-00OR22725 with Oak Ridge National Laboratory, managed and operated by UT-Battelle, LLC.

## References

1. Fenn, J. B.; Mann, M.; Meng, C. K.; Wong, S. F.; Whitehouse, C. M. Electrospray Ionization For Mass-Spectrometry of Large Biomolecules. *Science* **1989,** *246,* 64–71.
2. Karas, M.; Hillenkamp, F. Laser Desorption Ionization Of Proteins With Molecular Masses Exceeding 10,000 Daltons. *Anal. Chem.* **1988,** *60,* 2299–2301.
3. Liu, P.; Ziemann, P. J.; Kittelson, D. B.; McMurry, P. H. Generating Particle Beams of Controlled Dimensions and Divergence. 2. Experimental Evaluation of Particle Motion in Aerodynamic Lenses and Nozzle Expansions. *Aerosol. Sci. Technol.* **1995,** *22,* 314–324.
4. Beavis, R. C.; Chait, B. T. Velocity Distributions of Intact High Mass Polypeptide Molecule Ions Produced by Matrix Assisted Laser Desorption. *Chem. Phys. Lett.* **1991,** *181,* 479–484.
5. Friedlander, S. K. *Smoke, Dust, and Haze*; John Wiley and Sons, Inc.: New York, 1977.
6. Dawson, P. H., Ed. *Quadrupole Mass Spectrometry and Its Applications (American Vacuum Society Classics)*; AIP Press: Woodbury, NY, 1995.
7. Hayashi, T.; Sakudo, N. *International Conference on Mass Spectrometry*; Kyoto, Japan, 1969, p. 263.
8. Ding, L.; Sudakov, M.; Brancia, F. L.; Giles, R.; Kumashiro, S. A Digital Ion Trap Mass Spectrometer Coupled with Atmospheric Pressure Ion Sources. *J. Mass Spectrom.* **2004,** *39,* 471–484.
9. Wang, X. L.; Kruis, F. E.; McMurry, P. H. Aerodynamic Focusing of Nanoparticles: I. Guidelines for Designing Aerodynamic Lenses for Nanoparticles. *Aerosol. Sci. Technol.* **2005,** *39,* 611–623.
10. Eiceman, G. A.; Karpas, Z. *Ion mobility spectrometry*; CRC Press: Boca Raton, FL, 2005.
11. Bacher, G.; Szymanski, W. W.; Kaufman, S. L.; Zollner, P.; Blaas, D.; Allmaier, G. Charge-reduced nano-electrospray ionization combined with differential mobility analysis of peptides, proteins, glycoproteins, noncovalent protein complexes, and viruses. *J. Mass Spectrom.* **2001,** *36,* 1038–1052.
12. Dehmelt, H. G. Radiofrequency Spectroscopy of Stored Ions. *Adv. Atom. Mol. Phys.* **1967,** *3,* 53.